

# PARTICLE ACCELERATION ASSOCIATED WITH INTERACTING CORONAL MASS EJECTIONS

N.J. Lehtinen<sup>1</sup>, S. Pohjolainen<sup>1</sup>, E. Valtonen<sup>2</sup>, K. Huttunen-Heikinmaa<sup>2</sup>, and A.E. Hillaris<sup>3</sup>

<sup>1</sup>Tuorla Observatory, University of Turku, FI-21500, Finland, Email: nijole@utu.fi, silpoh@utu.fi

<sup>2</sup>Department of Physics, University of Turku, FI-20014 Turku, Finland, Email: eino.valtonen@utu.fi, kahehu@utu.fi

<sup>3</sup>Section of Astrophysics, Astronomy and Mechanics, Department of Physics, University of Athens, 15784 Panepistimiopolis Zografos, Athens, Greece, E-mail: ahilaris@phys.uoa.gr

## ABSTRACT

Two coronal mass ejections (CME1 and CME2) were observed on November 9, 2002. CME1 was estimated to start around 11 UT, directed to the Northwest with estimated average plane-of-the-sky speed of 530 km/s. CME2 was associated with a GOES M4.6 X-ray flare which started at 13:08 UT in AR0180 and was directed to the Southwest with estimated average speed of 1840 km/s. The two CMEs seem to interact around 13:50 UT and two groups of DH type III bursts are observed after it. The radio source locations observed by the Nançay Radioheliograph (NRH) at 14:05 UT at 164 MHz suggest that the radio emission might be originating from the area where the two CMEs interact over the western limb. The calculated proton onset time from the *SOHO* ERNE data is close to the estimated CME interaction time.

## 1. INTRODUCTION

Coronal mass ejections (CMEs) are large-scale structures carrying plasma and magnetic field from the Sun. CMEs are associated with flares, filament eruptions, shocks, radio bursts, solar energetic particle (SEP) events, and have been found to be the primary cause of geomagnetic disturbances and changes in the solar wind flow (see, e.g., Jing et al., 2004; Gopalswamy et al., 2002; Cliver et al., 1999; Reames, 1999; Gosling, 1997).

SEP events are believed to be accelerated in the lift-off phase of CMEs, which could include either acceleration in flaring processes (e.g., de Jager, 1986), or acceleration in coronal/interplanetary shocks (e.g., Reames, 1999), or presumably in both (e.g., Kocharov & Torsti, 2002). The role of CME interaction in SEP production has also been studied recently (e.g., Gopalswamy et al., 2002).

Type III bursts are caused by subrelativistic ( $\sim 1$  to  $\sim 50$  keV) electron streams travelling outward from the Sun at a speed of about  $0.1c$  to  $0.5c$  (see, e.g. Dulk, 1985). Particle acceleration can be flare-related (e.g. by magnetic reconnection) or due to shocks (e.g. bow shock of a fast CME).

Solar radio type II bursts are thought to be caused by MHD shock waves propagating through the corona

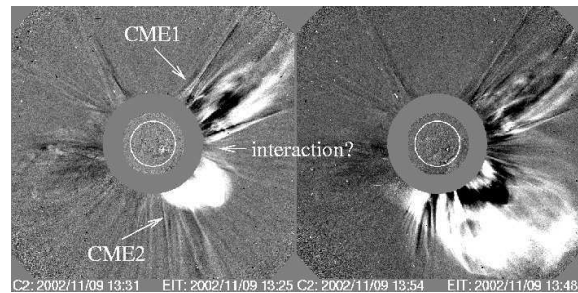


Figure 1. Two CMEs were observed on November 9, 2002. (LASCO CME Catalog, Catholic Univ. of America)

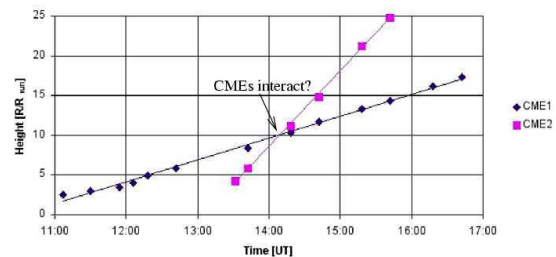


Figure 2. Height-time plots of CME1 and CME2. Both CMEs are at  $\sim 10 R_{sun}$  around 14:10 UT (data courtesy of LASCO CME Catalog).

and interplanetary medium (e.g. Nelson & Melrose, 1985). Shocks can be related to flare (blast) waves or be piston-driven bow shocks. There are some studies that suggest that coronal metric type II bursts and interplanetary (IP) decametric-hectometric (DH) type II bursts are not related at all (e.g., Cane & Erickson, 2005).

## 2. OBSERVATIONS AND DATA ANALYSIS

In this study we concentrate on analysing the white light images from *SOHO* LASCO (Brueckner et al., 1995) and

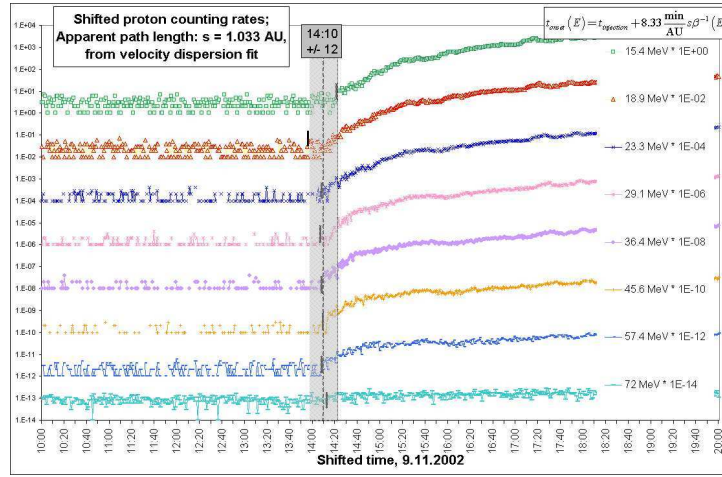


Figure 3. The proton counting rates observed by SOHO/ERNE. To separate the counting rates from each other, different series have been multiplied by suitable constants. The time series are plotted in shifted time by using path length  $s = 1.033$  AU, obtained from the velocity dispersion fit of protons (equation shown in the inset). The injection time near the Sun is marked by dashed, vertical line, and shaded area shows the error limits. To make the injection time comparable to the electromagnetic observations, eight minutes have to be added.

radio images at decimetric/metric wavelengths from the Nançay Radioheliograph (Kerdran & Delouis, 1997). We also use radio spectral data at decimetric/metric wavelengths from the Phoenix-2 at Zürich (Messmer, Benz, & Monstein, 1999) and Artemis-IV in Greece (Maroulis et al., 1997) and at decametric-hectometric wavelengths from the Wind/WAVES RAD2 (Bougeret et al., 1995).

On November 9, 2002 two CMEs (CME1 and CME2) were observed, see Fig.1. CME1 started before 11 UT and was directed to the NW with estimated average plane-of-the-sky speed of 530 km/s. CME2 was associated with a GOES M4.6 class X-ray flare which started around 13:08 UT and was directed to the SW with estimated average speed of 1840 km/s. The two CMEs are at a distance of  $\sim 10 R_{sun}$  around 14:10 UT (Fig.2). Interaction of the two CMEs is possible around 13:50 UT (interpolation between the available LASCO images at 13:31 and 13:54 UT).

An observable signature of SEP events is a velocity dispersion. Assuming that particles with different energies are released simultaneously at or close to the Sun, the onset of the event at 1 AU should be observed earlier at higher energies than at lower ones. Velocity dispersion analysis makes it possible to infer the release time of particles at the Sun and the apparent path length travelled. The onset time determination of SEP events and the method of velocity dispersion analysis in deriving the release time at the Sun were recently discussed by Huttunen-Heikinmaa et al. (2005, see also references therein).

Proton acceleration was estimated from SOHO ERNE

data by assuming a travel path of 1.033 AU, which is acquired from the velocity dispersion fit of ERNE protons to take place between 14:06 and 14:30 UT (see Fig.3). Electron acceleration was estimated from Wind and ACE in situ observations with the same presumptions to start between 13:43 and 13:59 UT.

The dynamic radio spectrum from Artemis-IV at 100–600 MHz shows narrow-band fluctuations one minute after the flare start and a drifting feature starting around 13:15 UT with frequency drift of about  $0.8 \text{ MHz}^{-1}$ , see Fig.4. The fluctuations might be due to trapped, accelerated electrons and the drifting feature might be due to a shock front or a preceding CME (indicates CME2).

The WAVES RAD2 measurements from the Wind satellite (see Fig.5) show IP type II burst around 13:32 UT at about 5 MHz that is probably due to the leading edge of the preceding CME2 and can be tracked in DH emission between 5 and 2 MHz. Local plasma density at 5 MHz corresponds to atmospheric height of about  $3.2 R_{sun}$  and at 2 MHz to about  $5.2 R_{sun}$  (Saito, 1970). The shock driver speed is estimated to be at least 1550 km/s. Different atmospheric density models give slightly different results, e.g. the equatorial density model by Demoulin & Klein (2000) gives an estimate of 2150 km/s.

We can see two separate DH type III groups in the dynamic spectra (see, Fig.5). The first group starts around 13:48 UT with starting frequency of  $\sim 60$  MHz. This corresponds to atmospheric height of  $0.6 R_{sun}$  above the photosphere. The start time of the first group is close to

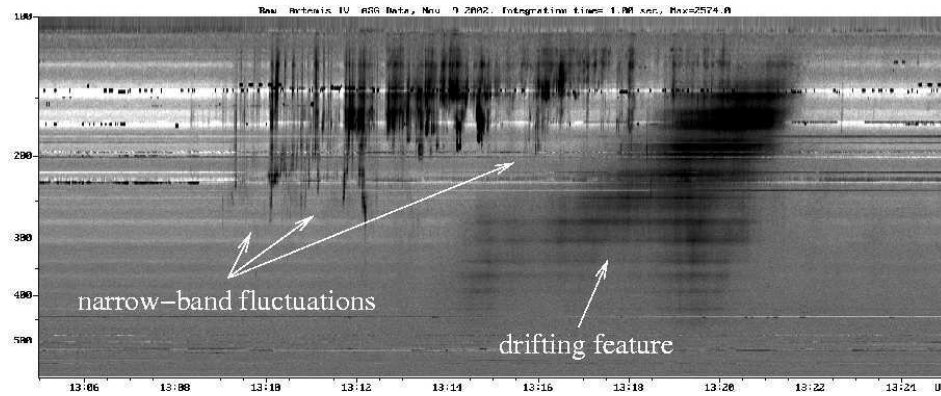


Figure 4. Artemis-IV spectrum at the frequency range 100–600 MHz at 13:05–13:25 UT shows narrow-band fluctuations and a drifting feature. The fluctuations might be due to trapped accelerated electrons. The drifting feature with a drift speed around 0.8 MHz/s might be due to a shock front or a preceding CME (timing indicates CME2).

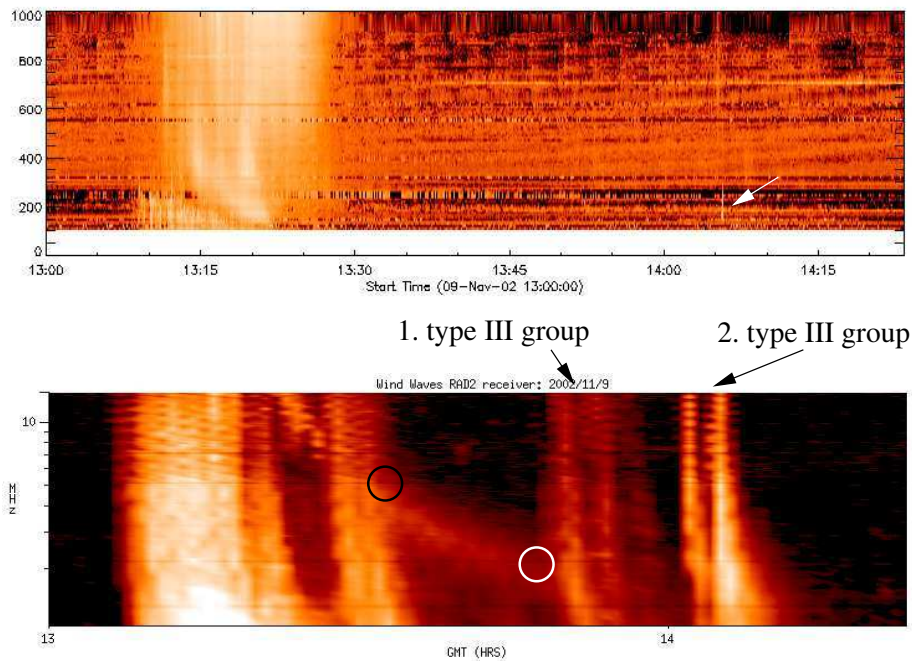


Figure 5. At the top: Phoenix-2 spectral plot from ETH Zurich at the frequency range 100–1000 MHz at 13:00–14:40 UT. At the bottom: Wind/WAVES RAD2 shows IP type II burst around 13:32 UT at about 5 MHz, indicated by a black circle. Around 13:48 UT, indicated by a white circle a group of type III bursts cross the type II lane. The first type III burst group has a starting frequency around 60 MHz (data not shown here; Nançay Decametric Array (DAM) observations at 70–20 MHz) and the second group around 250 MHz, indicated with a white arrow.

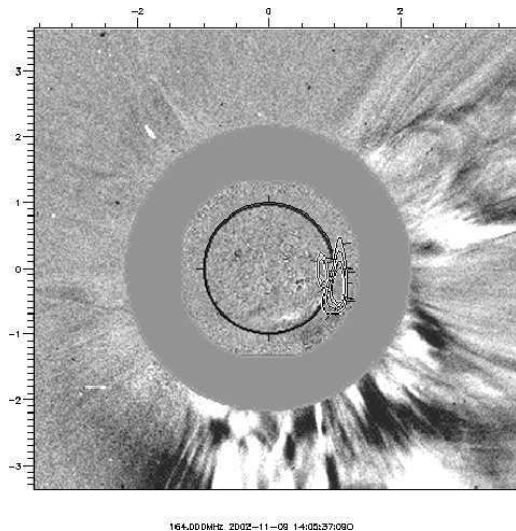


Figure 6. Radio burst locations observed by Nançay Radioheliograph (NRH) at 164 MHz at 14:05 UT.

the CME interaction time ( $\sim 13:50$  UT) and it takes place during the descending phase of the GOES X-ray flare. There are no observations of other flaring activity during this period. The second type III group starts at 14:02 UT in the *Wind*/WAVES RAD2 spectrum and in higher frequencies at  $\sim 14:05$  UT at 250 MHz in the ETHZ Phoenix-2 spectrum. The higher frequency indicates low atmospheric height of  $\sim 0.1 R_{sun}$ . The timing of the second group fits relatively well with proton acceleration times. It should be noted that no type III burst activity is seen in the spectra after the 14:05 burst group. Radio burst locations of the 14:05 UT emission observed by Nançay Radioheliograph (NRH) suggest that the radio emission might be originating from an area where the two CMEs partly interact, see Fig.6.

### 3. RESULTS

Analysis shows that the CMEs start to interact around 13:50 UT. Electron and proton acceleration might take place at coronal heights between 0.1 and  $0.6 R_{sun}$  after the flare maximum (13:25 UT) and could be caused by the interacting CMEs. Similar cases have been reported by Klein & Posner (2005) and their results of acceleration heights between 0.1 and  $0.5 R_{sun}$  agree with our estimations.

*Acknowledgements.* We thank the radio group at LESIA, Observatoire de Paris, France, for the use of Nançay

Radioheliograph data, the ACE EPAM instrument team, WIND 3DP instrument team, and the Coordinated Data Analysis Web (CDAWeb) for providing the ACE and WIND data. The LASCO CME Catalog is generated and maintained by NASA and Catholic University of America in co-operation with the Naval Research laboratory. *SOHO* is an international co-operation project between ESA and NASA. N.J.L. wishes to thank the Väisälä Foundation of the Finnish Academy Of Science and Letters for a travel grant to SPM-11.

### REFERENCES

- Bougeret J.-L., et al. *Space Sci. Rev.*, Vol. 71, 231-263, 1995
- Brueckner, G.E., Howard, R.A., Koomen, M.J., et al., *Sol.Phys.*, Vol. 162, 357-402, 1995
- Cane, H.V. & Erickson, W.C., *ApJ*, Vol. 623, 1180-1194, 2005
- Cliver, E.W., Webb, D.F., & Howard, R.A., *Sol.Phys.*, Vol. 187, 89-114, 1999
- Demoulin, P. & Klein, K.-L., *Transport and Energy Conversion in the Heliosphere, Lectures Given at the CNRS Summer School on Solar Astrophysics Oleron, France, 25-29 May 1998*, ed. Rozelot, J.P., Klein, L., & Vial, J.-C., Lecture Notes in Physics, Vol. 553, 99, 2000
- Dulk, G.A., *Ann. Rev. Astron. Astrophys.*, Vol. 23, 169-224, 1985
- Gopalswamy, N., Yashiro, S., Michalek, G., et al. *ApJ*, Vol. 572, 103-107, 2002
- Gosling, J.T. Coronal Mass Ejections, *Geophysical Monograph 99*, 9, 1997
- Huttunen-Heikinmaa, K., Valtonen, E., & Laitinen, T., *A&A*, manuscript no. aa2620-04, in press, 2005
- de Jager, C., *Space Sci. Rev.*, Vol. 44, 43-90, 1986
- Jing, J., Yurchyshyn, V.B., Yang, G., Xu, Y., & Wang, H., *ApJ*, Vol. 614, 1054-1062, 2004
- Kerdraon, A., & Delouis, J., *Coronal Physics from Radio and Space Observations; Proceedings of the CESRA Workshop*, ed. G. Trottet, Springer, 192, 1997
- Klein, K.-L. & Posner, A., *A&A*, Vol. 438, 1029-1042, 2005
- Kocharov, L. & Torsti, J., *Sol.Phys.*, Vol. 207, 149-157, 2002
- Maroulis, D., Dumas, G., Caroubalos, C., Bougeret, J.L., Moussas, X., Alissandrakis, C., & Patavalis, N., *Sol. Phys.*, Vol. 172, 353-360, 1997
- Messmer, P., Benz, A.O., & Monstein, C., *Sol. Phys.*, Vol. 187, 335-345, 1999
- Nelson, G.J. & Melrose, D.B. *Solar Radio Physics*, eds. D.J. McLean and N.R. Labrum, Cambridge Univ. Press, 333, 1985
- Reames, D.V., *Space Science Reviews*, Vol. 90, 413-491, 1999
- Saito, K., *Ann. Tokyo Astr. Obs.*, Vol. 12, 51-173, 1970